Effect of antifreeze protein on heterogeneous ice nucleation based on a two-dimensional random-field Ising model

Zhen Dong,[1] Jianjun Wang,[2,3] and Xin Zhou[1,*]

[1]*School of Physical Sciences, University of Chinese Academy of Science, Beijing 100049, People's Republic of China*

[2]*Key Laboratory of Green Printing, Institute of Chemistry, Chinese Academy of Sciences, Beijing 100190, People's Republic of China*

[3]*School of Chemistry and Chemical Engineering, University of Chinese Academy of Sciences, Beijing 100049, People's Republic of China*

(Received 25 January 2017; revised manuscript received 26 March 2017; published 25 May 2017)

Antifreeze proteins (AFPs) are the key biomolecules that protect many species from suffering the extreme conditions. Their unique properties of antifreezing provide the potential of a wide range of applications. Inspired by the present experimental approaches of creating an antifreeze surface by coating AFPs, here we present a two-dimensional random-field lattice Ising model to study the effect of AFPs on heterogeneous ice nucleation. The model shows that both the size and the free-energy effect of individual AFPs and their surface coverage dominate the antifreeze capacity of an AFP-coated surface. The simulation results are consistent with the recent experiments qualitatively, revealing the origin of the surprisingly low antifreeze capacity of an AFP-coated surface when the coverage is not particularly high as shown in experiment. These results will hopefully deepen our understanding of the antifreeze effects and thus be potentially useful for designing novel antifreeze coating materials based on biomolecules.

DOI: 10.1103/PhysRevE.95.052140

I. INTRODUCTION

Antifreeze proteins, also known as ice-binding proteins (IBPs), have the fascinating capacity of depressing the freezing temperature of water [1–5], which allows bacteria [6], fish [7], plants [8], and insects [9] to survive at temperatures even below 0 °C. This unique property of inhibiting water freezing provide the potential of a wide range of applications in the food industry [10–12] as well as in cryopreservation techniques [13,14], from conferring the freeze resistance of plants [15,16] to inhibition of gas clathrate formation [17,18], etc. Recently, by chemically coating AFPs onto various substrates, it was found that the surfaces were enabled to hinder the freezing of water on them more efficiently in comparison with a traditional hydrophilic polymer-coated surface [19,20]. This could provide a more efficient and environmentally friendly way to prevent or delay surface ice formation, which is a major problem in numerous applications such as aircrafts, power lines, air conditioners, wind turbines, etc. [21–24].

To explain the effects of AFPs, Raymond *et al.* developed a theory called adsorption-inhibition mechanism [25], which stated that the specific ice-binding face of AFPs in the solution binds to the surface of nascent ice crystals and the bound AFPs inhibit further growth and recrystallization of ice crystals due to the Kelvin effect [26,27]. Although the adsorption-inhibition mechanism is widely accepted to illustrate the antifreeze mechanism of AFPs in a solution or cell, it does not apply to the AFP-coating cases. Since all AFPs are attached to the surface with their ice-binding faces, they are not able to move and to bind to ice crystals. In a very recent experiment, Liu *et al.* coated the silicon substrate with AFPs by attaching the ice-binding face of AFPs onto the substrate and keeping the non-ice-binding face exposed to water [28]. The experiment discovered a surprisingly low antifreeze capacity of AFP-coated surface if the AFP coverage was not particularly high, and a sharp decrease in the freezing temperature of water only at relatively high coverage. This result is completely different from the free AFPs in solution, which have strong antifreeze capacity at low concentration [1,4,29], and raises a fascinating question of what is the origin of this low-coverage plateau of the AFP-coated surfaces.

In principle, molecular simulation is a good way to gain insights into this problem. However, due to the large size and the long time scale of this water-AFP-surface system, the traditional molecular dynamics simulation may require an extremely (if not impractical) high computational cost. Here, we present a coarse-grained two-dimensional (2D) random-field Ising model to simulate the freezing of water on the AFP-coated surface, which provides a mesoscopic understanding of heterogeneous ice nucleation. In this model, a thin layer of water on the water-substrate interface is described by a 2D lattice, and each AFP is represented as an external field, which acts locally on a small region of the lattice to decrease the difference of chemical potential between the ice and water and thus inhibits freezing. We demonstrate that the size of individual AFPs and their coverage on the coated surface, as well as the antifreeze capacity of each individual AFP dominates the freezing temperature of water. Our results show that the ice nucleation likely happens in gap regions of the surface without covering of AFPs. For low-coverage AFP-coated surfaces, there exists a large-enough gap region where an ice nucleus can grow up to critical size. Therefore, the ice nucleation that dominates the freezing temperature is not hindered by AFPs effectively. On high-coverage surfaces, due to the small size of gaps, the ice nucleation is hindered by the coated AFPs before the nucleus grows up to the critical size. The results provide a reasonable explanation for the low-coverage plateau found in experiments, and show that smaller-sized AFPs may have stronger antifreeze effects in comparison with larger-sized AFPs at the same coverage.

*xzhou@ucas.ac.cn

II. METHODS

The interfacial water on the substrate surface is represented by a 2D lattice. In this lattice model, each lattice site has two states, ice or water. The AFPs on the surface are considered to decrease the difference of chemical potential between ice and water, by mimicking the changed free-energy barrier of ice nucleation around the non-ice-binding face of the AFPs [5].

The free energy of the system presents as

$$G = G_i + G_{cp} + G_s. \tag{1}$$

G_i is the interaction energy of adjacent sites, from the interfacial free energy between ice and water. G_{cp} represents the chemical potential difference between ice and water, and G_s denotes the free-energy contribution of AFPs. The first term competes with the summation of the final two terms during the nucleation of ice.

For each lattice site i, we apply a discrete variable S_i equals to 1 or -1, indicating if the site i is water or ice, respectively. Another discrete variable A_i equals to 1 or 0, denoting if there is AFP covering the surface at the site i or not, 1 for covered and 0 for uncovered. Then, we have,

$$G_i = \frac{1}{2} g \sum_{\langle ij \rangle} (1 - S_i S_j), \tag{2}$$

where g is the ice-water interfacial free energy per each adjacent site. The summation is limited in all the pairs of adjacent sites.

G_{cp} can be written as

$$G_{cp} = \frac{1}{2} \Delta\mu \sum_i S_i, \tag{3}$$

where $\Delta\mu = \mu_{\text{ice}} - \mu_{\text{water}}$ is the chemical potential difference between ice and water at a single site. The $\Delta\mu$ can be transformed into $\Delta\mu = L_m(T_0 - T)/T_0$, where L_m is the latent heat of water freezing at a single site, and T is the temperature of system [30,31]. T_0 is the melting point of bulk water, here $T_0 = 273.15$ K.

G_s indicates the antifreeze property of AFPs on the surface, and

$$G_s = \frac{1}{2} \sum_i [\alpha A_i + \beta(1 - A_i)] S_i, \tag{4}$$

where α denotes the decrease of chemical potential difference between ice and water caused by AFPs, and β denotes the decrease caused by the AFP-uncovered surface.

The effect of AFPs and uncovered surface on ice and water described by G_s in Eq. (4) can be merged into G_{cp} in Eq. (3). We have,

$$G = -\frac{1}{2} g \sum_{\langle ij \rangle} S_i S_j + \sum_i h_i S_i, \tag{5}$$

where

$$h_i = \frac{L_m}{2T_0} [T_0 + T_\alpha A_i + T_\beta (1 - A_i) - T]. \tag{6}$$

Here we have already ignored the unimportant additive constant of the free energy in Eq. (5). In Eq. (6), $T_\alpha = \alpha T_0/L_m$ and $T_\beta = \beta T_0/L_m$ represent the shifting of freezing temperatures in the 2D model caused by AFPs and the uncovered substrate, respectively. The two sums in Eq. (5) correspond to the adjacent interaction and the external magnetic field in the well-known Ising model. For simplicity, we concentrate on the effect of AFPs, and the effect of the uncoated surface is ignored, thus here T_β is set as 0.

To estimate the parameter g and L_m, we consider each lattice site as a right square prism of water or ice, with the length of l and the height of h. Then, $g = lh\sigma$ and $L_m = l^2 h L_{m0}$, where σ is the interfacial tension between ice and water, and L_{m0} is the latent heat per unit volume. The interfacial tension σ is a parameter that can only be roughly estimated [31]. In the present simulation, we consider $\sigma = 25 \times 10^{-3}\ \text{Jm}^{-2}$. The other parameter latent heat is taken as $L_{m0} = 3.3 \times 10^8\ \text{Jm}^{-3}$. It should be noted that these two values are for the bulk water, which may be slightly different for the interfacial water. However, in the current case, we mainly focus on the effects of AFPs, which are not affected qualitatively by these two parameters, σ and L_{m0}, if they vary within a reasonable range.

For the geometric parameter l, since it only determines the way to cut the surface into a lattice, it is critical for simulation efficiency, but not related to the equilibrium properties of the system. In this work, we found $l = 2.5$ Å is a suitable value. The other geometric parameter h represents the thickness of the water layer we study, which is taken as 8 Å, containing about four solvation shells, slightly thicker than the hydration water layer around the nonbinding face of AFPs [5].

At the beginning of all simulations, AFPs are randomly placed according to various size, shape, and coverage settings. Using the Monte Carlo (MC) method to simulate a cooling process, we initiate the simulation at a relatively high temperature, at which the entire lattice is water. We run the system for 1000 MC turning attempts per lattice site in average, then lower the temperature by 0.1 K. We repeat this running and cooling procedure until the entire system turns into ice, then we get the freezing temperature where half of the system is frozen during each individual simulation. We repeat the simulation 100 times by randomly resetting the AFP locations on the substrates to calculate the mean freezing temperature. The size of lattice is 720×720, a slight adjustment would be implemented if AFPs of some specific sizes and shapes are not able to cover the entire lattice, and the lattice model is presented with periodic boundaries.

III. RESULTS AND DISCUSSION

The mean value of S_i of all sites, M, is calculated for every simulation step, and the average of M at each temperature in a typical cooling process is shown in Fig. 1. $(M + 1)/2$ gives the fraction of ice in lattice. The M-temperature figures of all simulations share the same graphic feature of Fig. 1, as the curve drops sharply near the freezing temperature. The model shows the property of first-order phase transition, the same as the real water freezing process. Also the same as real water, even for the AFP-uncovered surface, the nucleation can only happen at a supercooling temperature below the melting point in simulation. The temperature at which $\overline{M} = 0$ is considered as the freezing point of the system.

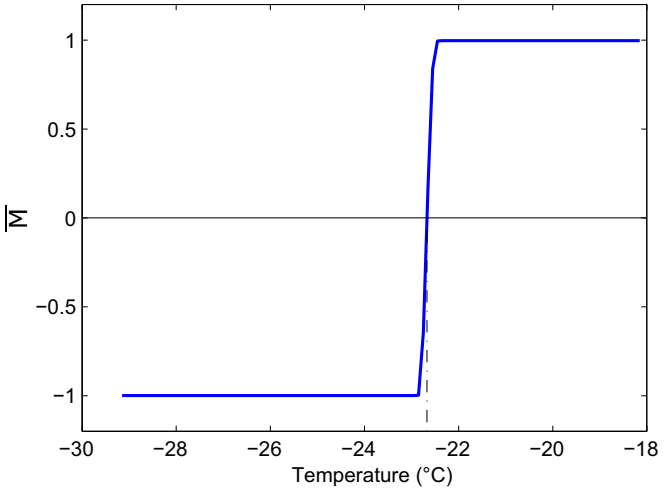

FIG. 1. The average of M at each temperature in a typical cooling process. M is the mean value of all S_i at each MC step. Here, the freezing temperature is calculated as $-22.7\,^{\circ}$C.

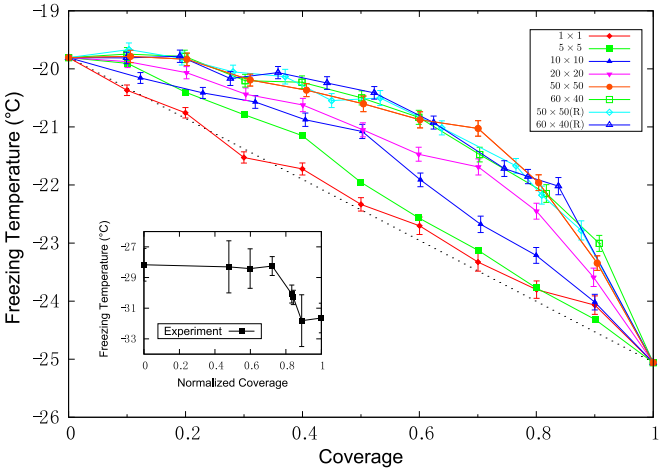

FIG. 2. The freezing temperature of water on surfaces covered with AFPs of various sizes and shapes at different coverage. In the main figure, the size of AFPs range from single site (1×1) to rectangle (60×40), and the letter R indicates the AFPs have random orientation. The straight dotted line is from the mean-field theory. Here, $T_\alpha = 5.6\,^{\circ}$C. The inset is replotted from the experimental result presented by Liu *et al.* [28].

From a microscopic point of view, for all simulations, in the early stages of the cooling processes, a few isolated ice sites appear, mostly in the areas that are not covered by AFPs, but usually disappear after some MC steps. As the temperature is decreased to the freezing point, many small adjacent ice sites begin to emerge into groups, occasionally to form one big ice nucleus, i.e., an ice nucleation event happens. If the ice sites group can grow larger than the critical nucleus, it will develop rapidly and end up freezing the entire system. The size of critical nucleus of the system can be estimated by classical nucleation theory. In the temperature range studied, the critical nucleus contains about 6–7 lattice sites in diameter, corresponding to a free-energy barrier of about 20 k_BT.

In order to study the antifreeze properties of AFPs, the effects of the size of AFPs, the cooling rate of system, and T_α are investigated in the following.

A. Effect of AFP sizes

The antifreeze capacity of AFPs of various sizes at different coverage are shown in Fig. 2. The freezing-temperature-coverage curve of particularly small AFPs is close to a straight line, while the curve gradually becomes more convex upward as the AFPs become larger. For small-sized AFPs, the freezing temperature of water on AFP-coated surface decreases in proportion to coverage. However, for large-sized AFPs, they show very little antifreeze capacity at low coverage.

The result of a recent experiment relevant to our simulation work is shown in inset of Fig. 2 [28]. In the experiment, by measuring the freezing temperature of tiny water droplets on an AFP-coated substrate of various coverage, a freezing-temperature-coverage curve was obtained. The experimental normalized coverage was calculated from the mass of AFPs deposited on substrate. The calculated normalized coverage is slightly different from the theoretical coverage in simulation at extremely high coverage because in reality the AFPs cannot cover the entire surface without leaving any gaps, and the mass increase of coated AFPs may be due to a few overlaps. In general, our simulation results of large-sized AFPs agree well with their experimental result qualitatively. The coated surface shows little antifreeze capacity at a low AFP coverage, while the freezing-temperature-coverage curve declines drastically at high coverage.

In order to study the microscopic antifreeze mechanism, four typical ice nucleation events on surfaces covered by AFPs with same coverage but different sizes and shapes are shown in Fig. 3. On a surface covered by relatively large-sized AFPs such as 50×50 or 60×40, an ice nucleus can easily form and grow in the gap between AFPs, as shown in Figs. 3(a)–3(c). When this ice nucleus grows to the AFP-covered area, its size is considerably larger than the critical size, and the free energy of the system declines sharply as it grows. Under this circumstance, the antifreeze effect of AFPs is limited. Their antifreeze capacity mainly reflects in reducing the nucleation rates by restricting the possible nucleation area.

To investigate the effect of shape and the orientation degrees of freedom of AFPs, we simulate AFPs as squares and rectangles, with and without rotation. The size of the rectangular AFPs is 60×40, whose area is similar to that of the square AFPs with size of 50×50. In rotational cases, the orientation of every AFP is randomly chosen from 12 possible ones. As shown in Fig. 2, these three curves almost coincide with the curve of the square AFPs (50×50) without rotation, indicating that the shape change and orientation degrees of freedom are of little significance for the antifreeze capacity of AFPs on surface. This result confirms our explanation of the antifreeze mechanism that the antifreeze capacity of the AFP-covered surface is dominated by the distribution of gaps between AFPs, since the shape, square or rectangular, and the orientational freedom do not change the gap distribution substantially.

However, on a surface covered by small-sized AFPs, the spacing areas between AFPs are too small for the ice nucleus to grow. As a result, the ice nucleus extends to many

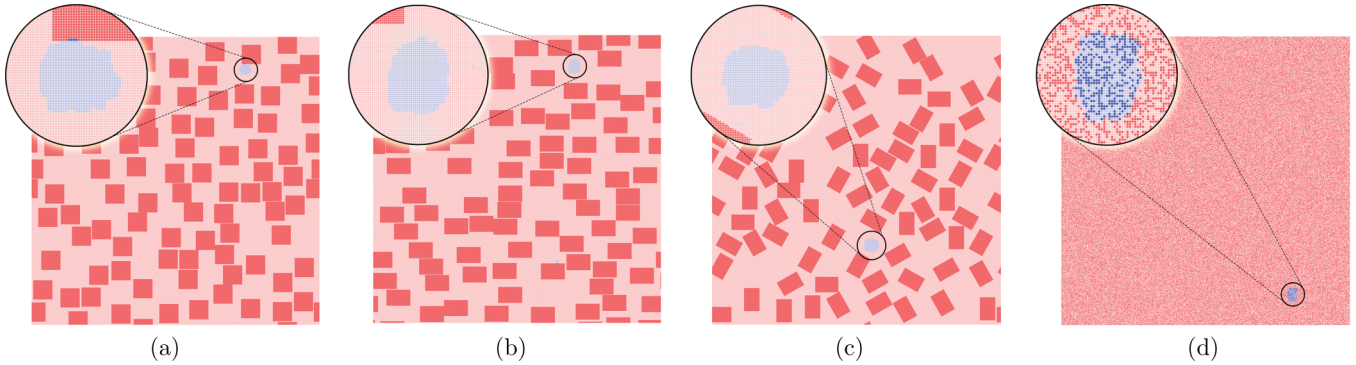

FIG. 3. Four typical ice nucleation events when substrate surface is covered by AFPs of different sizes and shapes but at the same coverage 40%. The surface is represented in pink, and the attached AFPs are indicated by red squares or rectangles. The blue color represents ice. Specifically, the light blue indicates ice on uncovered surface, and the dark blue represents ice on the top of AFPs. Water is considered to be transparent. The four types of AFPs in are: (a) square AFPs of size 50×50 (lattice sites), (b) rectangular AFPs of size 60×40, (c) rectangular AFPs of the same size as in (b) but having random orientation, and (d) pointlike AFPs each covering only single site. The entire panel consists of 750×750 sites in (a), and consists of 720×720 lattice sites in (b), (c), and (d).

AFP-covered sites when growing, as shown in Fig. 3(d). Under these circumstances, the effect of randomly placed discrete external fields appears to be a uniform mean field. So A_i, which equals to 0 or 1 representing the covering state of AFPs on site i, can be replaced by a uniform continuous variable, the coverage of AFPs, C. It is equivalent to reset the bulk melting temperature in Eq. (6) as a linear function of C. Then, we approximately have a linear freezing temperature on the coverage from $C = 0$–1, which is consistent with the simulation results of small-sized AFPs.

Based on our simulation results and analysis above, the ice formation in the gap between AFPs is the origin of the low-coverage plateau in the experimental result. For large-sized AFPs in simulation, since each lattice site is considered to be a right square prism with the length l of 2.5 Å, and the magnitude of the real AFP size is several nanometers, it is quite reasonable that in the simulation model the large-sized AFPs, which contain dozens of sites but not the small-sized AFPs may offer a much better description of the real systems.

B. Effect of the cooling rate

In our simulations, the cooling process takes a step-down approach, which lowers the temperature by 0.1 K after 1000 MC turning attempts per lattice site in average. To confirm that this nonequilibrium process is slow enough, we do simulations with 10 times slower cooling rate, i.e., each lattice site takes 10000 turning attempts in average at every temperature. The freezing-temperature-coverage curves at both cooling rates are shown in Fig. 4. For the AFP-coated

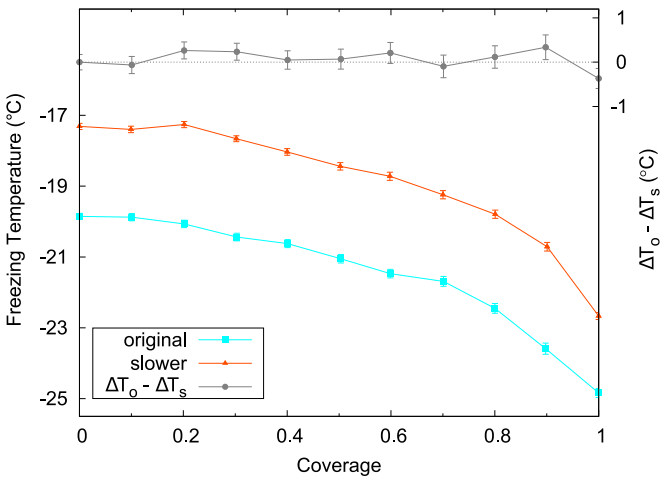

FIG. 4. The freezing temperature at different cooling rates. Each lattice site takes 1000 MC turning attempts in average at original cooling rate (cyan line), and takes 10000 at the slower cooling rate (red line). The difference between ΔT_o (ΔT at the original cooling rate) and ΔT_s (ΔT at the slower cooling rate) are calculated, as shown by the gray line. The size of AFPs is 20×20 in both simulations, and $T_\alpha = 5.6\,^\circ$C.

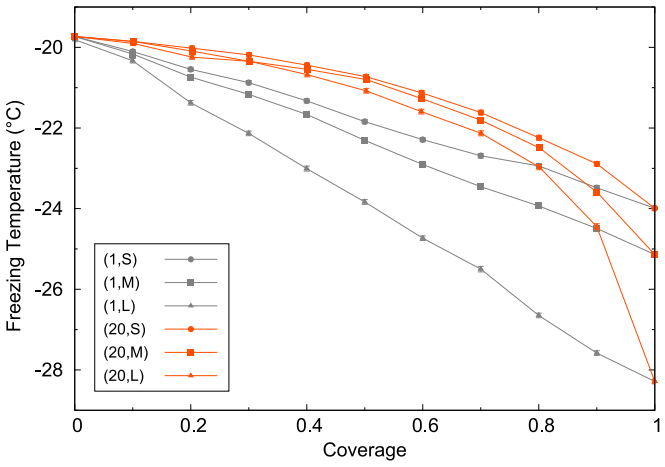

FIG. 5. The freezing temperature of water on surfaces covered with square AFPs of different sizes and T_α. In the legend: number indicates the length of AFP square lattice, and letter indicates the relative magnitude of T_α small (S), medium (M), or large (L). The three parameters are $T_{\alpha,\text{small}} = 4.5\,^\circ$C, $T_{\alpha,\text{medium}} = 5.6\,^\circ$C, and $T_{\alpha,\text{large}} = 9.0\,^\circ$C. Here each freezing temperature is averaged from 500 independent simulations at the same condition but different random realization of AFP positions, without considering the orientation degrees of freedom of AFPs.

TABLE I. The simulational and theoretical resutls of freezing temperature depression ΔT for surfaces fully covered by AFPs with different T_α. The unit of values in the table is °C.

ΔT	Small	Medium	Large
Simulational	4.4 ± 0.1	5.4 ± 0.1	8.4 ± 0.1
Theoretical	4.5	5.6	9.0

surface, the antifreeze effect of AFPs can be represented by the freezing temperature depression ΔT, which is the difference between the freezing temperature of water on AFP-covered and noncovered surfaces. In order to investigate the effect of the slower cooling rate, the difference between ΔT of the two simulations (of the original and the slower cooling rate) is calculated. As shown by gray line in Fig. 4, ΔT remains unchanged for the slower simulation, and the freezing temperature shift of water on the noncovered surface is not related to our explanation for the antifreeze mechanism of AFPs. So we conclude that the original cooling rate is slow enough to avoid the nonequilibrium effect on our conclusions.

C. Effect of the parameter T_α

While the difference in antifreeze capacity of different-sized AFPs is due to the influence of the AFP population, the parameter T_α reflects the antifreeze capacity of individual AFPs. The freezing-temperature-coverage curves of two different size AFPs with three different T_α are shown in Fig. 5. For the same-sized AFPs, the freezing temperature decreases with T_α proportionally, and the shape of the curves is straight for the small-sized AFPs and convex for the larger ones.

In order to check the compatibility of simulation and theory, the simulation results and theoretical value of freezing temperature depression ΔT at AFP full-covered surface are calculated, as shown in Table I. The theoretical value of ΔT for a full-covered surface is $T_\alpha - T_\beta$. The simulational results shown in the table are consistent with the theoretical.

IV. CONCLUSIONS

Inspired by the latest experimental approaches of creating an antifreeze surface by coating with AFPs [19,20], we present a two-dimensional lattice model to investigate the effect of AFPs on heterogeneous ice nucleation. The simulation results show that the antifreeze capacity of an AFP-coated surface depends on coverage strongly. The antifreeze capacity of AFPs changes from colligative to noncolligative as size increases. For small-sized AFPs, the freezing temperature depression of the AFP-coated surface increases in proportion to coverage; the effect of AFPs can be considered as a mean field. However, for large-sized AFPs, the antifreeze capacity is restrained due to the large gap area between them, which weakens the antifreeze capacity of a low-coverage coating surface. The results are consistent with the recent experiments, and provide a reasonable explanation for the surprisingly low antifreeze capacity of an AFP-coated surface if the coverage is particularly high. Moreover, a crucial factor, the amount of free-energy change of water in the solvation shells outside the AFP non-ice-binding face, as α in the context, is estimated, which may be useful in theorety or experiments in the future. Furthermore, the understanding of the antifreeze mechanisms of the AFP-coated surface presented here would certainly benefit the antifreeze industries.

It should be pointed out that there are some limitations of the 2D model. Since the real system is three dimensional, a 3D Ising model might be more accurate and more general to study ice freezing in more complicated environments, such as in AFP-covered rugged surfaces. The model we present here would only apply to a geometrically smooth AFP-covered surface.

Although we are able to gain a global view of antifreezing through this lattice model, all molecular details are missing unfortunately. There have been many more accurate molecular dynamics simulation studies on AFPs [5,32–34], however, they all focus on a very small scale, usually a single protein or even a part of it. In our coarse-grained model, not only the antifreeze properties of individual proteins, but also the behavior of the protein population are studied. Our results indicate that at least the initiation of freezing, the nucleation process, might be able to be studied by MD simulation, since it happens in a small local spatial region. Therefore, although the present coarse-grained lattice model loses the molecular details, it provides a mesoscopic understanding of freezing, and might be useful to combine with some local MD simulations in the future to investigate the more precise details.

ACKNOWLEDGMENTS

The work is supported by the National Natural Science Foundation of China (NSFC), Grant No. 11574310. We are very grateful to Cheng Yang, Fei Yuan Yongshun Song, and Professor Ming Li for fruitful discussions, and to Shun Xu for providing lattice visual plug-in of VMD.

[1] M. Bar Dolev, I. Braslavsky, and P. L. Davies, Ann. Rev. Biochem. **85**, 515 (2016).
[2] P. Scholander, L. van Dam, J. Kanwisher, H. Hammel, and M. Gordon, J. Cell. Comp. Physiol. **49**, 5 (1957).
[3] A. L. DeVries and D. E. Wohlschlag, Science **163**, 1073 (1969).
[4] Y. Yeh and R. E. Feeney, Chem. Rev. **96**, 601 (1996).
[5] D. R. Nutt and J. C. Smith, J. Am. Chem. Soc. **130**, 13066 (2008).
[6] H. Kawahara, Y. Nakano, K. Omiya, N. Muryoi, J. Nishikawa, and H. Obata, J. Biosci. Bioeng. **98**, 220 (2004).
[7] P. L. Davies and C. L. Hew, FASEB J. **4**, 2460 (1990).
[8] M. Griffith and M. W. Yaish, Trends Plant Sci. **9**, 399 (2004).
[9] E. Kristiansen, C. Wilkens, B. Vincents, D. Friis, A. B. Lorentzen, H. Jenssen, A. Løbner-Olesen, and H. Ramløv, J. Insect Physiol. **58**, 1502 (2012).
[10] S. Payne, D. Sandford, A. Harris, and O. Young, Meat Sci. **37**, 429 (1994).

[11] K. Cook and R. Hartel, Comp. Rev. Food Sci. Safety **9**, 213 (2010).
[12] N. S. Ustun and S. Turhan, J. Food Proc. Pres. **39**, 3189 (2015).
[13] A. Ideta, Y. Aoyagi, K. Tsuchiya, Y. Nakamura, K. Hayama, A. Shirasawa, K. Sakaguchi, N. Tominaga, Y. Nishimiya, and S. Tsuda, J. Repro. Dev. **61**, 1 (2015).
[14] G. Amir, B. Rubinsky, S. Y. Basheer, L. Horowitz, L. Jonathan, M. S. Feinberg, A. K. Smolinsky, and J. Lavee, J. Heart Lung Transplant. **24**, 1915 (2005).
[15] G. Breton, J. Danyluk, F. Ouellet, and F. Sarhan, Biotechnol. Ann. Rev. **6**, 59 (2000).
[16] H. K. Khanna and G. E. Daggard, Plant Cell Rep. **25**, 1336 (2006).
[17] H. Ohno, R. Susilo, R. Gordienko, J. Ripmeester, and V. K. Walker, Chem. Eur. J. **16**, 10409 (2010).
[18] S. A. Bagherzadeh, S. Alavi, J. A. Ripmeester, and P. Englezos, Phys. Chem. Chem. Phys. **17**, 9984 (2015).
[19] A. P. Esser-Kahn, V. Trang, and M. B. Francis, J. Am. Chem. Soc. **132**, 13264 (2010).
[20] Y. Gwak, J.-i. Park, M. Kim, H. S. Kim, M. J. Kwon, S. J. Oh, Y.-P. Kim, and E. Jin, Sci. Rep. **5**, 12019 (2015).
[21] R. Gent, N. Dart, and J. Cansdale, Philos. T. Roy. Soc. A **358**, 2873 (2000).
[22] J. Laforte, M. Allaire, and J. Laflamme, Atmos. Res. **46**, 143 (1998).
[23] T. Li, D. Donadio, L. M. Ghiringhelli, and G. Galli, Nature Mater. **8**, 726 (2009).
[24] S. Jung, M. K. Tiwari, N. V. Doan, and D. Poulikakos, Nature Commun. **3**, 615 (2012).
[25] J. A. Raymond and A. L. DeVries, Proc. Natl. Acad. Sci. USA **74**, 2589 (1977).
[26] J. J. Thomson, *Applications of Dynamics to Physics and Chemistry* (Macmillan, London, 1888), p. 251.
[27] W. Kuhn, Helv. Chim. Acta **39**, 1071 (1956).
[28] K. Liu, C. Wang, J. Ma, G. Shi, X. Yao, H. Fang, Y. Song, and J. Wang, Proc. Natl. Acad. Sci. USA **113**, 14739 (2016).
[29] D. Wen and R. A. Laursen, J. Biol. Chem. **267**, 14102 (1992).
[30] M. K. Yau and R. Rogers, *A Short Course in Cloud Physics* (Elsevier, Amsterdam, 1996), pp. 12–14.
[31] L. Ickes, A. Welti, C. Hoose, and U. Lohmann, Phys. Chem. Chem. Phys. **17**, 5514 (2015).
[32] R. K. Kar and A. Bhunia, Prog. Biophys. Mol. Bio. **119**, 194 (2015).
[33] A. Kuffel, D. Czapiewski, and J. Zielkiewicz, J. Chem. Phys. **143**, 135102 (2015).
[34] H. Nada and Y. Furukawa, Phys. Chem. Chem. Phys. **13**, 19936 (2011).